JOC The Journal of Organic Chemistry

ARTICLE

pubs.acs.org/joc

Substituent Effects on the Reversibility of Furan−Maleimide Cycloadditions

Robert C. Boutelle and Brian H. Northrop*

Department of Chemistry, Wesleyan University, Middletown, Connecticut 06459, United States

Supporting Information

ABSTRACT: The effects of furan and maleimide substitution on the dynamic reversibility of their Diels−Alder reactivity have been investigated computationally and by ^{1}H NMR spectroscopy. Furan and furan derivatives bearing methoxy, methyl, or formyl groups at their 2- or 3-positions were investigated with maleimide and maleimide derivatives bearing *N*-methyl, *N*-allyl, and *N*-phenyl substituents. Computational predictions indicate that electronic and regiochemical effects of furan substitution significantly influence their Diels−Alder reactivity with maleimide, with reaction free energies of exo adduct formation ranging from $\Delta G = -9.4$ to 0.9 kcal/mol and transition state barriers to exo adduct formation ranging from $\Delta G^{\ddagger} = 18.9$ to 25.6 kcal/mol. Much less variation was observed for the reactivity of N-substituted maleimide derivatives and furan, with reaction and transition state free energies each falling within a range of 1.1 kcal/mol. Dynamic exchange experiments monitored by ^{1}H NMR spectroscopy support computational predictions. The results indicate the reactivity and reversibility of furan−maleimide cycloadditions can be tuned significantly through the addition of appropriate substituents and have implications in the use of furan and maleimide derivatives in the construction of thermally responsive organic materials.

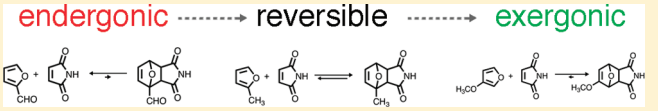

INTRODUCTION

Dynamically reversible covalent bond forming reactions have been the subject of increasing interest over the past two decades, largely because of their relevance to biological chemistry, molecular and macromolecular materials, and supramolecular chemistry. Dynamic covalent reactions proceed via relatively low activation barriers and form products that are only slightly exergonic relative to starting reagents, thus allowing the reverse reaction to also take place under appropriate conditions. The potential for both forward and reverse reactivity allows for the construction of dynamic combinatorial libraries (DCLs)[1,2] and forms the basis of dynamic covalent chemistry (DCC),[3−5] wherein mixtures of multiple components undergo continual exchange under thermodynamic equilibrium conditions. Examples of dynamic covalent reactions include imine condensations, aldol exchange, transesterifications, disulfide formation, boronic ester condensations, and alkene metathesis. Dynamic covalent exchange provides a means of adaptive proofreading as kinetic intermediates are cycled through en route to the most thermodynamically stable product (or products). Similar concepts of dynamic reversibility have been exploited for over half a century in the context of noncovalent self-assembly.[6−10] Dynamic covalent chemistry has the advantage of combining the reversibility of noncovalent self-assembly with the strength of covalent bond formation. This adaptability, ease of synthesis, and product stability has made dynamic covalent chemistry particularly well suited to the construction of organic materials.

Many early applications of DCC focused on the formation of synthetic receptors utilizing imine, ester, disulfide, and acetal chemistries.[11] Template-directed dynamic assembly[12−15] has enabled the efficient construction of various materials ranging from colloids[14] and coordination complexes[13] to mechanically interlocked molecules such as rotaxanes,[16] catenanes,[17] suitanes,[18] Borromean rings,[19] and Solomon knots.[20] More recently several research groups[21−24] have used the reversible condensation of boronate esters to assemble a variety of covalent organic frameworks (COFs) with applications in gas uptake and storage, organic photovoltaics, and catalysis. Severin[25] and Nitschke[26] have demonstrated the simultaneous use of two or more dynamic covalent reactions in the synthesis of macrocycles and capsules.

It has been known for over 50 years that some Diels−Alder reactions can be made reversible.[27] The application of reversible Diels−Alder chemistry to the dynamic covalent assembly of organic materials, however, has only recently been explored.[28−40] This comes despite the fact that Diels−Alder reactions have the desirable property of being self-contained: i.e., all atoms present in the starting diene and dienophile are present in the resulting adduct. The equilibrium position of reversible Diels−Alder reactions, therefore, responds to temperature, solvent, and concentration but is not influenced by ancillary molecules such as water in the case of imine and boronic ester condensations or transition-metal catalysts in the case of alkene metathesis. The number of Diels−Alder reactions that undergo dynamically reversible adduct formation under mild conditions is, however, limited and there is increasing interest in expanding the set of dynamic covalent Diels−Alder reactions.[41−44]

Over the past 10 years several groups have explored the use of reversible Diels−Alder adduct formation in the design and

Received: August 1, 2011
Published: August 26, 2011

dx.doi.org/10.1021/jo201606z | *J. Org. Chem.* 2011, 76, 7994–8002

Scheme 1. Parent [4 + 2] Cycloaddition of Unsubstituted Furan with Maleimide To Give the Kinetic Endo and Thermodynamic Exo Diels–Alder Adducts

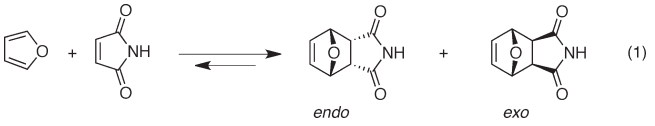

synthesis of new organic materials. The majority of such studies utilize the reactivity of electron-rich furan derivatives with electron-poor maleimide derivatives. The [4 + 2] cycloaddition of furan and maleimide can be accomplished at or slightly above room temperature, while the retrocyclization is accomplished at elevated temperatures (Scheme 1). Wudl and co-workers have developed transparent organic polymers that, when cracked, are thermally remendable on account of reversible furan–maleimide cycloadditions.[28] Similar demonstrations of the utility of furan–maleimide cycloadditions in the preparation of molecular materials include thermally reversible dendrimers and dendronized polymers,[29−31] surfactants,[32] epoxy resins,[33] cross-linked polymer networks,[34−36] and the aggregation[37] and manipulation[38,39] of gold nanoparticles. Each of the preceding examples involve furan compounds that are mono- or disubstituted with alkyl, ether, ester, or amine substituents. It is well-known[27,31,45] that the substitution of furans greatly effects their reactivity with dienophiles, such as maleimide. Despite this sensitivity to substitution, and the increasing application of furan–maleimide cycloadditions to materials development, there have yet to be any systematic investigations of the effects of furan and maleimide substitution on the thermodynamics of their Diels–Alder reactivity.

We report herein computational and spectroscopic investigations of the electronic and regiochemical effects of furan substitution on the reversibility of furan–maleimide cycloaddition reactions and discuss their implications on the use of dynamic furan–maleimide cycloadditions in materials synthesis. The results show that, with the appropriate substituents, furan–maleimide cycloadditions can be tuned along a scale ranging from exergonic to dynamically reversible to endergonic.

RESULTS AND DISCUSSION

Diels–Alder cycloaddition reactions of furan and maleimide have been studied both experimentally[46−48] and computationally.[49] Furan–maleimide adduct formation proceeds to give exo and endo products, with the exo species being the thermodynamic product and endo the kinetic. Rickborn et al. report[50] that, in the case of furan reacting with *N*-methylmaleimide at 40 °C in acetonitrile solution, the exo isomer is more stable than the endo by 1.8 kcal/mol (reaction 2, Scheme 2). In the same study the authors investigated the cycloaddition of isobenzofuran with *N*-methylmaleimide (reaction 3, Scheme 2). Adduct formation in reaction 3 involves the formation of a stable aromatic product and is therefore considerably more favorable. The thermodynamic equilibrium for the reaction of isobenzofuran and *N*-methylmaleimide therefore requires heating at 132 °C in chlorobenzene in order to observe reversibility. The authors determined a $\Delta\Delta G_{endo\text{-}exo}$ value of 2.4 kcal/mol. Computational methods presented herein were benchmarked against these experimental studies in order to test their appropriateness, and the results are shown in Table 1. Density functional methods at the B3LYP/6-311 g(d,p) level deviated significantly from experimental values in the gas phase in solvent models for both acetonitrile and chlorobenzene. This observation is consistent with prior computational research that has shown B3LYP methods to be accurate[51] for pericyclic reactions involving hydrocarbons but unreliable[45] for pericyclic reactions involving heteroatoms. More computationally intensive MP2 and CBS methods, on the other hand, proved significantly more accurate.

The best agreements with experimental results were achieved utilizing single-point electronic energies obtained at the MP2/6-311+G(d,p) level with vibrational frequency analysis carried out at the CBS-QB3 level. Transition states were optimized similarly,

Table 1. Experimental and Calculated Reaction (ΔG) and Transition State ($\Delta G^{\ddagger}$) Free Energies for Diels–Alder Cycloadditions between Furan and *N*-Methylmaleimide (Reaction 2) and between Isobenzofuran and *N*-Methylmaleimide (Reaction 3) Used To Benchmark Computational Methods[a]

	Reaction 2							
	exptl		computational[a]					
	CH_3CN/313 K		in vacuo/298 K		CH_3CN/298 K		CH_3CN/313 K	
	ΔG	$\Delta G^{\ddagger}$	ΔG	$\Delta G^{\ddagger}$	ΔG	$\Delta G^{\ddagger}$	ΔG	$\Delta G^{\ddagger}$
endo	−1.9	24.9	−2.0	22.4	−1.5	22.5	−1.3	23.1
exo	−3.7	25.2	−4.1	22.6	−4.5	22.7	−4.4	23.4
	Reaction 3							
	exptl		computational					
	PhCl/405 K		in vacuo/298 K		PhCl/298 K		PhCl/405 K	
	ΔG	$\Delta G^{\ddagger}$	ΔG	$\Delta G^{\ddagger}$	ΔG	$\Delta G^{\ddagger}$	ΔG	$\Delta G^{\ddagger}$
endo	−17.1	18.2			−25.7	9.2	−19.6	14.3
exo	−19.5	19.4			−26.5	10.4	−20.4	15.2

[a] All values are in kcal/mol.

Scheme 2. Diels-Alder Cycloaddition Reactions between Furan and *N*-Methylmaleimide (Reaction 2) and between Isobenzofuran and N-Methylmaleimide (Reaction 3), the Dynamic Reversibility of Which Have Been Studied Experimentally

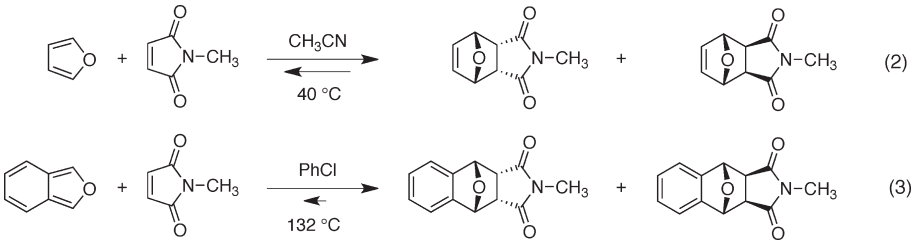

dx.doi.org/10.1021/jo201606z |J. Org. Chem. 2011, 76, 7994–8002

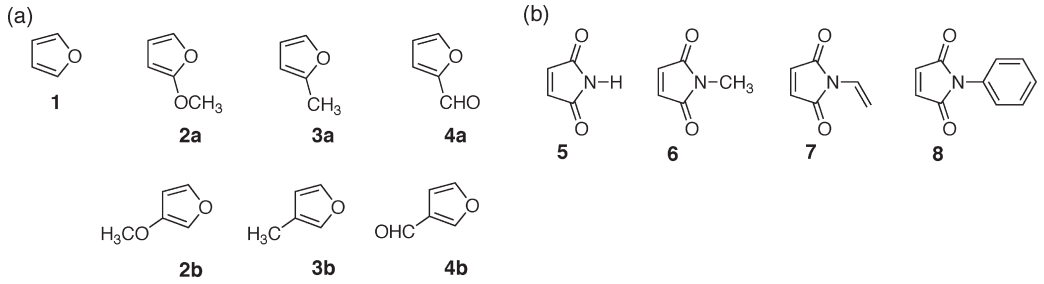

Figure 1. Chemical structures of the substituted furan (a) and maleimide (b) derivatives investigated in the present study.

though using less computationally intensive MP2/6-31+G(d) electronic energies. Reaction and transition state free energies were obtained in the gas phase at 298 K, solvated in either CH_3CN or PhCl at 298 K, and solvated at experimental temperatures (313 or 405 K). Computations accurately predict the endo isomer to be favored kinetically and the exo isomer to be favored thermodynamically in each case for reactions 2 and 3. The closest agreement between calculated and experimental reaction and transition state free energies for the reaction of furan with *N*-methylmaleimide, reaction 2, was obtained when including solvent and correcting for the experimental temperature. Calculated reaction free energies in this case are within 0.7 kcal/mol of experimental values. Calculations accurately reproduce the experimentally observed difference in transition state free energies of $\Delta\Delta G^{\ddagger}_{\text{endo-exo}}$ = 0.3 kcal/mol for reaction 2, while absolute predictions of the exo and endo transition state free energies are within 1.2 kcal/mol. Likewise, correcting for solvent and experimental temperatures gave the best agreement for the reaction of isobenzofuran with *N*-methylmaleimide (reaction 3). Calculated reaction free energies for this reaction deviate from experimental values to a greater extent in absolute terms (0.9−2.5 kcal/mol), though they still reproduce experimental trends. With these benchmarking studies at hand, the effects of furan and maleimide substitution on their Diels−Alder reactivity were then investigated.

Figure 1 shows the series of substituted furan and maleimide compounds chosen for this study. Furan and furan derivatives with a methoxy, formyl, and methyl substituent at either the 2- or 3-position were investigated. This particular series was chosen for their widely varying electronic character (electron donating, withdrawing, and alkyl) as well as the commercial availability of most compounds in the series. In the current study only monosubstituted furan derivatives were investigated. Maleimide and maleimide derivatives with methyl, vinyl, and phenyl substituents were also studied.

Electronic Effects. Table 2 summarizes the calculated reaction and transition state energies and free energies for Diels−Alder cycloadditions between furan (**1**) and maleimide (**5**) as well as between furan derivatives **2a**,**b**−**4a**,**b** and maleimide derivatives **6**−**8**. It is well-known that Diels−Alder cycloadditions involving electron-rich dienes and electron-poor dienophiles proceed more favorably.[27,45] This trend is borne out across the series of compounds investigated computationally. The effects of adding alkoxy, alkyl, and aldehyde sutstibutents to furan, whether at the 2- or 3-position, generally follow what would be expected, given their Hammett parameters. The greatest increase in exergonicity of adduct formation is seen with the most electron donating methoxy substituent. In the case of 2-methoxyfuran (**2a**), formation of the exo adduct with maleimide is predicted to proceed with ΔG = −6.0 kcal/mol. This value is 2.4 kcal/mol more favorable than the parent reaction with unsubstituted furan. The effect is even greater in the case of 3-methoxyfuran (**2b**), where adduct formation is predicted to be favored by −9.4 kcal/mol, which is 5.8 kcal/mol more favorable than the parent reaction with unsubstituted furan. In addition to increasing the reaction free energy, methoxy substitution lowers the transition state free energy barrier to adduct formation relative to unsubstituted furan (**1**) by 1.5−2.2 kcal/mol. While methoxy substitution is predicted to both increase the exergonicity of and lower the barrier to adduct formation, computations predict the greater effect is seen in the overall reaction free energy: i.e. the effect is more pronounced for ΔG than for $\Delta G^{\ddagger}$. These results predict that the addition of strongly electron donating substituents to furan should *decrease* their utility as partners with maleimide in

Table 2. Calculated Reaction Enthalpies (ΔH), Transition State Enthalpies ($\Delta H^{\ddagger}$), Reaction Free Energies (ΔG), and Transition State Free Energies ($\Delta G^{\ddagger}$) (kcal/mol) for Furan−Maleimide Diels−Alder Cycloadditions

furan	maleimide	product	isomer	ΔH	$\Delta H^{\ddagger}$	ΔG	$\Delta G^{\ddagger}$	ΔG_{MeCN}	$\Delta G^{\ddagger}_{\text{MeCN}}$
1	**5**	**9**	endo	−16.0	9.4	−1.2	23.1	−1.1	23.0
			exo	−18.1	9.5	−3.3	23.2	−3.6	23.0
2a	**5**	**10**	endo	−21.9	6.6	−5.8	21.3	−5.9	20.5
			exo	−22.6	6.3	−6.4	21.3	−6.0	20.8
2b	**5**	**11**	endo	−22.3	5.8	−7.4	19.6	−7.5	18.9
			exo	−24.2	6.4	−9.4	20.0	−9.4	19.3
3a	**5**	**12**	endo	−18.0	7.2	−2.7	21.4	−2.4	21.3
			exo	−19.3	7.6	−4.0	21.6	−4.0	21.6
3b	**5**	**13**	endo	−18.9	6.8	−3.9	20.8	−3.6	20.9
			exo	−20.3	7.7	−5.4	21.3	−5.8	21.0
4a	**5**	**14**	endo	−11.4	12.1	3.2	25.9	3.5	25.6
			exo	−14.4	11.3	0.3	25.1	0.9	25.4
4b	**5**	**15**	endo	−14.1	10.4	0.5	24.1	1.0	24.8
			exo	−18.0	10.4	−3.4	24.0	−3.7	24.3
1	**6**	**16**	endo	−17.3	8.7	−3.0	22.4	−1.5	22.5
			exo	−19.2	9.0	−4.5	22.6	−4.5	22.7
1	**7**	**17**	endo	−16.5	8.1	−1.7	21.9	−1.4	21.9
			exo	−18.4	8.7	−3.6	22.5	−3.8	22.1
1	**8**	**18**	endo	−16.7	8.0	−2.0	21.9	−2.4	21.8
			exo	−18.5	8.7	−3.8	22.3	−4.8	21.6

dynamic covalent chemical applications. The significantly lower reaction free energies result in high barriers to retrocyclization: e.g., the cycloaddition of 3-methoxyfuran (**2b**) with maleimide (**5**) to give the product **11**-*exo* has $\Delta G^{\ddagger} = 19.3$ kcal/mol, whereas its retrocyclization requires $\Delta G^{\ddagger} = 28.7$ kcal/mol.

Methyl substitution is also predicted to increase the favorability of adduct formation, though to a lesser extent. Reacting 2-methylfuran (**3a**) with maleimide (**5**) lowers the free energy of endo and exo product formation by 1.3 and 0.4 kcal/mol, respectively. This increase in favorability increases slightly when 3-methylfuran (**3b**) is used as the starting diene, with endo and exo product formation predicted to be more favorable by 2.5 and 2.2 kcal/mol, respectively, relative to unsubstituted furan. Calculated free energy barriers to the formation of Diels–Alder adducts between methylfurans and maleimide are lower than the corresponding barriers for the parent adducts by 1.4–1.7 kcal/mol, in the case of 2-methylfuran, and 2.0–2.1 kcal/mol, in the case of 3-methylfuran. It is therefore predicted that the increased favorability of adduct formation is, within error, balanced out by a decrease in the free energy barrier to adduct formation.

In effect, alkyl substitution provides a means of developing more complex and synthetically useful furan dienes to be used as partners with maleimide dienophiles in dynamic covalent chemical applications without disrupting the dynamic reversibility of Diels–Alder adduct formation. These results are especially important given the increasing number of examples wherein furan dienes, substituted at either the 2-position or the 3-position with either alkyl groups or alkyl ethers, have been used in conjunction with maleimide derivatives for the dynamic covalent synthesis of organic materials such as surfactants, polymers, and dendrimers. Indeed, Kakkar et al. have experimentally observed[31] the differences in reactivity of furans substituted at their 2-position with either alkyl or ester functionalities: 2-alkyl furans underwent reversible Diels–Alder reactions with maleimides to give thermoresponsive dendrimers, whereas direct substitution with electron-poor ester functionalities resulted in furans that were unreactive toward maleimides. These experimental observations are in agreement with the computational predictions presented herein. Furthermore, it is predicted that while both 2- and 3-methylfuran will react reversibly with maleimide at high temperatures, alkyl substitution at the 3-position will result in a more stable, more robust Diels–Alder adduct on return to ambient temperatures. Such subtle distinctions are important for the development of, for example, thermally remendable polymers.

Interestingly, and somewhat counterintuitively, computations predict the addition of an electron-withdrawing aldehyde substituent to furan results in either endergonic or exergonic Diels–Alder reactivity with maleimide, depending on the regiochemistry of furan substitution. Reacting maleimide with 2-furaldehyde (**4a**) is predicted to be endergonic by 3.5 and 0.9 kcal/mol for endo and exo isomers, respectively. The same reaction with 3-furaldehyde (**4b**), on the other hand, is predicted to be endergonic by 1.0 kcal/mol in the case of the endo adduct and exergonic by 3.7 kcal/mol in the case of exo adduct formation. This significant distinction again highlights the notable difference in reactivity of furans substituted at the 2-position and those substituted at the 3-position. Across the series of furan derivatives studied, those substituted at the 3-position react with maleimide to give exo Diels–Alder adducts that are 1.8–4.8 kcal/mol more favored than their corresponding 2-substituted isomers. This difference is greatest in the case of 2-furaldehyde versus 3-furaldehyde.

Table 3. Calculated Reaction Enthalpies for the Reactions between Furan and Dimethyl Ether, Ethane, and Acetaldehyde To Produce either a 2- or 3-Substituted Furan and Methane[a]

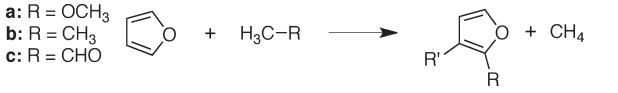

Reaction		$\Delta H_{(2\text{-sub})}$	Reaction		$\Delta H_{(3\text{-sub})}$	$\Delta H_{(3\text{-sub})\text{-}(2\text{-sub})}$
(4a)		-9.5	(5a)		-6.6	2.9
(4b)		-8.4	(5b)		-5.7	2.7
(4c)		-8.2	(5c)		-7.4	0.8

[a] Enthalpies are given in kcal/mol.

Aldehyde substitution is predicted to increase the free energy barriers to adduct formation by 1.3–2.6 kcal/mol relative to an unsubstituted furan. These results are generally supportive of the precedent that electron-poor dienes, such as **4a**, react less favorably with electron-poor dienophiles than electron-rich dienes, such as **2b**. It is surprising, however, that the electron-poor diene furan **4b** is predicted to react as favorably with maleimide **5** as is the unsubstituted and more electron rich parent furan **1**. This notable difference in predicted reactivity necessitated a more thorough investigation of the regiochemical effects of furan substitution.

Regiochemical Effects. The results of Table 2 indicate that furan substitution at the 3-position consistently leads to more negative reaction free energies and lower transition state barriers than substitution at the 2-position. This effect is present across the series of substituted furans **2**–**4** and is most pronounced in the case of aldehyde substitution. Isodesmic reactions were used to determine the origin of this increased favorability of adduct formation involving 3-substituted furans.

As can be seen in Table 3, isodesmic reactions corresponding to substitution of furan relative to methyl are exothermic in all cases, though they are more exothermic for substitution at the 2-position than at the 3-position. The 2-position of unsubstituted furan is more electropositive than the 3-position, which explains why substitution at the 2-position is most favored in the case of methoxy (reaction 4a, $\Delta H = -9.5$ kcal/mol), the strongest donating substituent. This also explains the differences in favorability between substitution at the 2-position versus 3-position ($\Delta\Delta H_{(3\text{-sub})-(2\text{-sub})}$) across the three substituents investigated, which is smallest for the most withdrawing aldehyde substituent (reactions 5c–4c, 0.8 kcal/mol) and greatest for the most donating methoxy (reactions 5a–4a, 2.9 kcal/mol). The overall trend in Table 2 indicates that the 3-substituted regioisomer of a given substituent is destabilized relative to the 2-substituted regioisomer. This difference ultimately plays an important role in the Diels–Alder reactivity of substituted furans with maleimide.

Isodesmic reactions in Table 4 were used to evaluate the effects of substitution on the furan–maleimide Diels–Alder adduct. Adduct formation has the two prominent effects of (i) alkylation at the 2- and 5-positions of the furan moiety and (ii) changing the π-system of the furan moiety from a 2,4-diene to a 3-alkene. These changes in alkylation and conjugation alter the trends in substituent favorability, as can be seen by comparing related isodesmic reactions in Tables 3 and 4. Methoxy substitution,

dx.doi.org/10.1021/jo201606z |J. Org. Chem. 2011, 76, 7994–8002

Table 4. Calculated Reaction Enthalpies for the Reactions between Furan−Maleimide Diels-Alder Adduct 9 and Dimethyl Ether, Ethane, and Acetaldehyde To Produce the Indicated 2- or 3-Substituted Adduct and Methane[a]

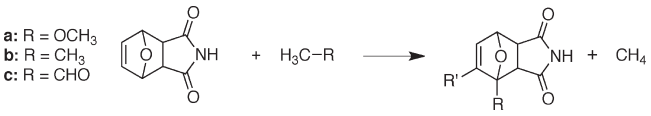

Reaction		$\Delta H_{(2\text{-sub})}$ endo	exo	Reaction		$\Delta H_{(3\text{-sub})}$ endo	exo
(6a)		-15.5	-14.1	(7a)	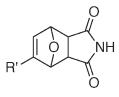	-13.0	-12.7
(6b)		-10.4	-9.6	(7b)		-8.6	-7.9
(6c)		-3.6	-4.5	(7c)		-5.5	-7.4

[a] Enthalpies are given in kcal/mol.

for example, is 4.6−6.4 kcal/mol more favorable in reactions 6a and 7a than in reactions 4a and 5a. This effect appears to be primarily the result of the change in conjugation rather than increased alkylation, given that the increases in reaction exothermicities on going from Table 3 to Table 4 are roughly the same whether methoxy substitution occurs at the 2-position (comparing reactions 4a and 6a) or the 3-position (comparing reactions 5a and 7a). Methyl substitution in reactions 6b and 7b shows only a modest increase in exothermicity of 1.2−2.9 kcal/mol relative to reactions 4b and 5b. For both methoxy and methyl substituents, substitution of the Diels−Alder adduct at the 2-position of the furan moiety is predicted to be more favorable than substitution at the 3-position, a trend also observed in Table 3.

In the case of aldehyde substition this preference is reversed: i.e., substitution at the 3-position of the furan moiety is more exothermic than that at the 2-position (Table 4). This role reversal can be explained by the fact that aldehyde substitution at the 3-position retains π-conjugation between the adduct and the aldehyde C═O, which is lost for aldehyde substitution at the 2-position. Taken together, the results presented in Tables 3 and 4 show that aldehyde substitution at the 2-position of furan (reaction 4c) is stabilized relative to substitution at the 3-position (reaction 5c), whereas the Diels−Alder adduct in reaction 6c is destabilized relative to the Diels−Alder adduct in reaction 7c. The increase in favorability of aldehyde substitution of the Diels−Alder adduct at the 3-position (1.9−2.9 kcal/mol) outweighs the 0.8 kcal/mol destabilization of aldehyde substitution of furan at the 3-position relative to the 2-position (Table 3). The difference in predicted reactivity between 2-furaldehyde and 3-furaldehyde with maleimide can therefore be attributed to two main factors: (i) aldehyde substitution at the more electropositive 2-position is less favorable than at the 3-position and (ii) the loss of π-conjugation upon Diels−Alder adduct formation in the case of 2-furaldehyde further disfavors adduct formation, whereas π-conjugation is retained in the case of 3-furaldehyde. The enthalpic effects investigated in isodesmic reactions of Tables 3 and 4 are able to support the predicted though counterintuitive reaction free energies presented in Table 2: namely, that formation of an exo Diels−Alder adduct between 3-furaldehyde and maleimide is predicted to be exothermic despite the electron-withdrawing nature of the aldehyde substituent. In the case of 2-furaldehyde reacting with maleimide, both exo and endo adduct formation is endothermic and unfavorable. Indeed, reacting

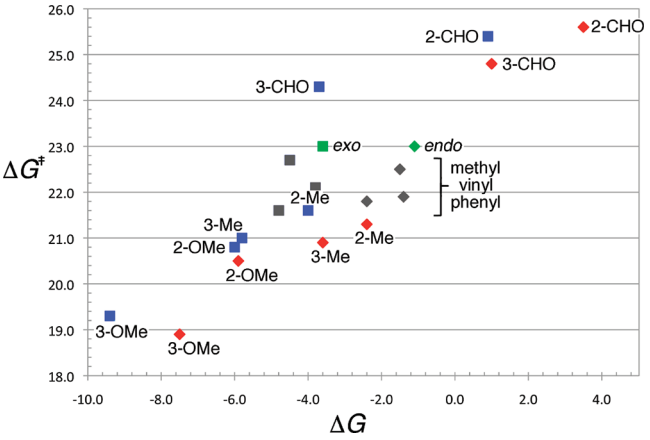

Figure 2. Plot comparing calculated reaction free energies (ΔG, x axis) and transition state free energies ($\Delta G^{\ddagger}$, y axis) in acetonitrile for furan−maleimide Diels−Alder cycloadditions investigated in this study. Endo isomers are symbolized by diamonds, while exo isomers are symbolized by squares. Adducts containing substituted furans are shown in either red (endo) or blue (exo) and labeled according to their substitution. Adducts containing substituted maleimides are shown in gray. Endo and exo adducts of the unsubstituted furan−maleimide Diels−Alder adduct are shown in green.

3-furaldehyde with maleimide results in the formation of minor amounts of adduct **15** (see the Supporting Information), whereas all attempts to react 2-furaldehyde with maleimide to give adduct **14** resulted in no reaction, in line with the predicted results.

Computational results presented herein suggest that the reactivity and reversibility of Diels−Alder reactions between substituted furans and maleimide can be tuned through the addition of appropriate substituents. Adduct formation can range from being strongly exergonic and thus irreversible (e.g., the reaction of 3-methoxyfuran **2b** with maleimide **5**) to slightly exergonic with increased reversibility (e.g., the reaction of 2-methylfuran **3a** with maleimide **5**) to endergonic (e.g., the reaction of 2-furaldehyde **4a** with maleimide **5**). These results have significant implications for the use of furan−maleimide cycloadditions in the dynamic covalent synthesis of organic materials. While methoxy substitution is predicted to lower the barrier to adduct formation and result in more stable Diels−Alder adducts, this favorability comes at the cost of significantly hindering reversibility.

Maleimide substitution was also investigated, and the results are presented in Table 2. The reactivity of N-alkyl-, N-allyl-, and N-phenyl-substituted maleimides with furan were studied. Substitution of maleimide dienophiles is predicted to have a less pronounced effect on reaction and transition state energetics than substitution of furan dienes. Overall, all three substituted maleimides increase the exergonicity of Diels−Alder adduct formation relative to unsubstituted maleimide by 0.2−1.3 kcal/mol, with methyl substitution showing the greatest effect. Maleimide substitution is also predicted to lower free energy barriers to adduct formation by 0.3−1.4 kcal/mol. While the effects of maldimide substitution are not as large or as variable as the effects of furan substitution, it is notable that the predicted decrease in transition state barriers is, within error, equal to the decrease in reaction free energies. It can therefore be expected that the addition of alkyl or aromatic groups to maleimide will not hinder but, rather, will likely facilitate their use in dynamic covalent chemical applications with furan and furan derivatives

dx.doi.org/10.1021/jo201606z |J. Org. Chem. 2011, 76, 7994–8002

Scheme 3. Dynamic Exchange Reactions Involving the Exchange of Maleimide (a) or Furan (b) Moieties Studied by ^{1}H NMR Spectroscopy

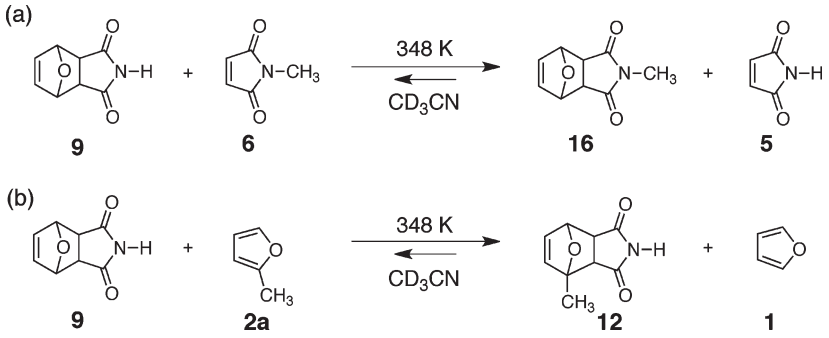

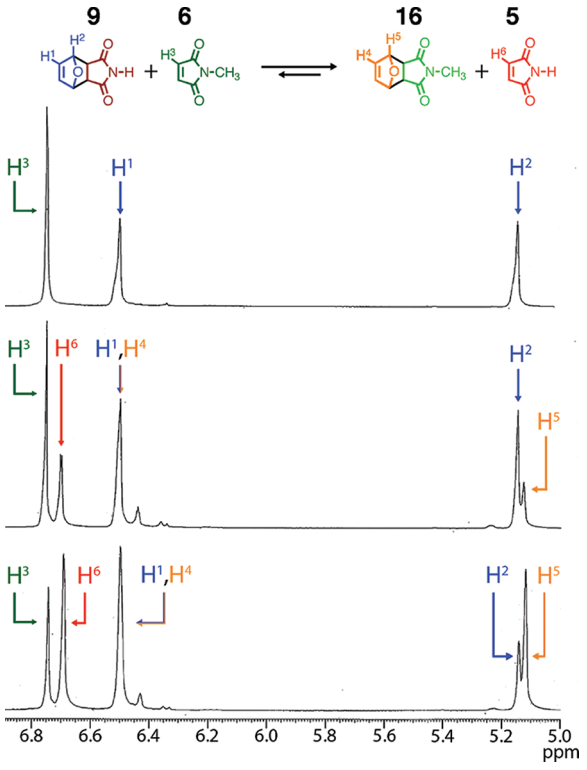

Figure 3. Partial ^{1}H NMR spectra recorded at t = 0 h (top), t = 51 h (middle), and t = 400 h (bottom), demonstrating maleimide/*N*-methylmaleimide exchange and equilibration between adducts **9** and **16**.

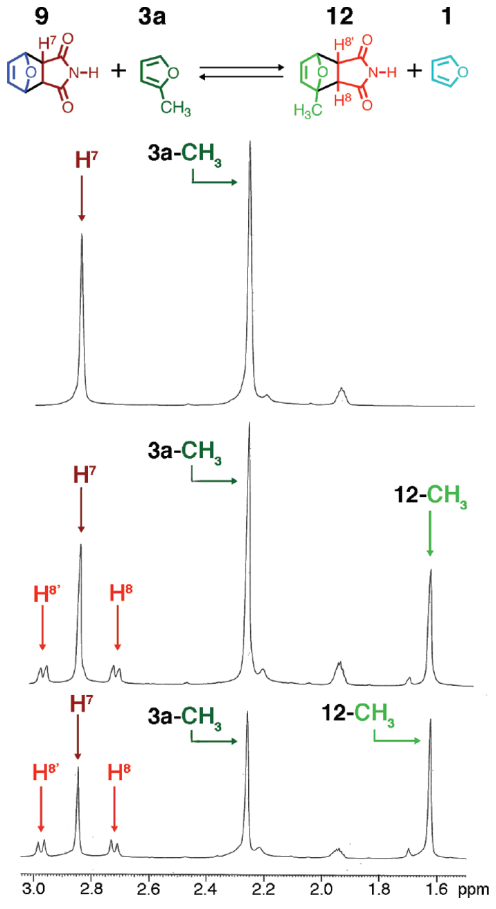

Figure 4. Partial ^{1}H NMR spectra recorded at t = 0 h (top), t = 93 h (middle), and t = 400 h (bottom), demonstrating furan/2-methylfuran exchange and equilibration of adducts **9** and **12**.

by slightly increasing the thermodynamic favorability of Diels–Alder adduct formation without significantly changing the kinetics of dynamic exchange.

Figure 2 summarizes the key results and predictions of the computational investigations reported herein. Computed reaction free energies (ΔG) and transition state free energies ($\Delta G^{\ddagger}$) for Diels–Alder cycloadditions for each furan/maleimide combination solvated in acetonitrile are plotted along the x and y axes, respectively. Endo isomers of Diels–Alder products are indicated by diamonds, while exo isomers of Diels–Alder products are represented as squares. Products of the parent reaction between furan and maleimide are shown in green. Diels–Alder adducts involving substituted maleimide (*N*-methyl, *N*-vinyl, or *N*-phenyl) are shown in gray. In all other cases endo isomers are further distinguished as being red, while exo isomers are blue. Several notable trends can be ascertained from the plotted reaction and transition state free energies: (i) in all cases the exo isomer is the thermodynamic product, as indicated by a more negative ΔG; (ii) in all cases except aldehyde substitution the endo isomer is the kinetic product, as indicated by a lower $\Delta G^{\ddagger}$ value; (iii) reactions between maleimide and 3-substituted furans invariably lead to both more stable Diels–Alder adducts and lower transition state barriers than the same reaction with the

dx.doi.org/10.1021/jo201606z |*J. Org. Chem.* 2011, 76, 7994–8002

corresponding 2-substituted furan; (iv) there is little variability (≤1.0 kcal/mol) in the Diels−Alder reactivity of furan with *N*-alkyl, *N*-vinyl, or *N*-phenyl maleimide; (v) the Diels−Alder reactivity of maleimide with substituted furans varies considerably, depending on the electronic character of the furan substituent and whether the substituent is attached at the 2- or 3-position of furan.

^{1}H NMR Spectroscopy. With the above computational predictions at hand, it became of interest to experimentally study the dynamic reversibility of furan−maleimide Diels−Alder reactivity through exhange reactions. Two dynamic exchange reactions were investigated spectroscopically: (i) exchange of the maleimide moiety of adduct **9** with *N*-methylmaleimide (Scheme 3a) and (ii) exchange of the furan moiety of adduct **9** with 2-methylfuran (Scheme 3b). For the dynamic exchange outlined in Scheme 3a, computations predict an equilibrium ratio of 22:78 between adducts **9** and **16**, given the relative stabilities of their exo and endo adducts computed in acetonitrile at 348 K.[52] A 0.25 M solution of furan−maleimide adduct **9** and *N*-methylmaleimide **6** in CD_3CN was prepared in a screw-top NMR tube and heated at 75 °C. Spectra were periodically recorded to monitor the extent of maleimide exchange. Figure 3 shows a time sequence of ^{1}H NMR spectra demonstrating the dynamic covalent exchange of maleimide with *N*-methylmaleimide. At 0.25 M and 75 °C the exchange requires approximately 320 h (see the Supporting Information). Heating a more concentrated sample (2.0 M) of the same 1:1 mixture at 100 °C allows the same equilibrium to be reached overnight as opposed to requiring 8 days. As previously stated, dynamic covalent Diels−Alder reactions are self-contained and only depend on temperature, concentration, and solvent. Spectroscopically the ratio of furan−maleimide adduct **9** and furan−*N*-methylmaleimide adduct **16** is 36:64, as determined by integration of well-isolated signals corresponding to hydrogen atoms H^3 and H^6 (Figure 3). This experimentally measured ratio is in good agreement with the computational prediction that *N*-methylmaleimide forms a more stable adduct with furan than maleimide does; however, experimental results do suggest computations may overestimate the stability of adduct **16** relative to **9**. Given the exponential relationship between percent contribution and relative free energy, a small error in computed free energies can have a significant effect on the predicted product ratios. Even so, the computationally predicted ratio agrees quite well with the experimental adduct ratio and, most importantly, computations and experiment agree that adduct **16** is more stable than adduct **9**.

Scheme 3b outlines the exchange of the unsubstituted furan moiety of adduct **9** with 2-methylfuran **3a**. Computations in Table 3 predict the exo and endo isomers of 2-methylfuran−maleimide adduct **12** to be 0.4 and 1.3 kcal/mol more stable, respectively, than the exo and endo isomers of unsubstituted furan−maleimide adduct **5**. The ratio of adducts **5** and **12** at equilibrium is therefore predicted to be 35:65. A 0.25 M CD_3CN solution containing equimolar amounts of furan−maleimide adduct **9** and 2-methylfuran **3a** was sealed in a screw-cap NMR tube and heated at 75 °C. Periodic monitoring of the $H^{7'}$ proton signal of furan−maleimide adduct **9** and the H^8 and $H^{8'}$ proton signals of 2-methylfuran−maleimide adduct **12** by ^{1}H NMR spectroscopy indicated equilibrium was reached after 260 h (see the Supporting Information). Again, a more concentrated sample can be equilibrated overnight at 100 °C. Integration of protons H^7 and $H^{8+8'}$ in Scheme 3b indicates an equilibrium ration of 50:50 between adducts **12** and **9**. The spectroscopic ratio is in general agreement with the computationally predicted ratio.

It is notable that the exchange of 2-methylfuran **3a** with furan **1** occurs faster than exchange of *N*-methylmaleimide **6** with maleimide **5**. This experimental observation is in line with the computationally predicted relative ratios of free energy barriers for these reactions. Specifically, the barriers to cycloaddition of 2-methylfuran **3a** with maleimide **5** are predicted to be 1.1−1.7 kcal/mol lower than the barriers to cycloaddition of unsubstituted furan with maleimide (**5**) or unsubstituted furan with *N*-methylmaleimide (**6**). Transition state free energies of the last two cycloaddition reactions—unsubstituted furan **1** reacting with either maleimide **5** or *N*-methylmaleimide **6**—are identical within error (±0.5 kcal/mol). The observation that maleimide exchange (Figure 3) is observed to require a longer time to reach equilibrium than furan exchange (Figure 4) supports the computationally predicted trend in free energy cycloaddition barriers.

These two representative examples of exchange processes demonstrate the utility and practicality of dynamic exchange involving substituted derivatives of furan dienes and maleimide dienophiles. They lend support to the computational predictions in this study and serve to further highlight the influences of furan and maleimide substitution on the dynamic reversibility of their Diels−Alder reactivity.

Conclusions. The importance of dynamic covalent chemistry to materials organic synthesis has been well established and continues to generate increasing interest. The application of reversible Diels−Alder reactions in the dynamic covalent synthesis of organic materials has only recently been explored. The results presented herein provide valuable insight into the electronic and regiochemical effects of furan and maleimide substitution on their applicability in dynamic covalent applications. Care must be taken when selecting which diene and dienophile combinations are used in dynamic covalent chemical applications, as differences in their electronic characteristics and substitution of the furan dienes at the 2- or 3-position greatly effect their reaction and transition state energetics. Even with the relatively limited series of monosubstituted derivatives studied herein, it can be shown that furan−maleimide reactivity can be tuned across a considerable range of reactivity: varying from largely exergonic and therefore irreversible reactions to mildly exergonic reactions with favorable exchange kinetics to unfavorable endergonic reactions. Selection of appropriate subsituents can help optimize materials properties, depending on whether increased reversibility, decreased reversibility, or particular exchange reactions are desired for a particular application. Given the increasing use of these systems in mendable macromolecules, such differences can have, and are already being shown to have, pronounced implications on material properties. Further investigations of a wider range of substituents, disubstituted compounds, and additional dynamic exchange competition studies are underway.

COMPUTATIONAL AND EXPERIMENTAL METHODS

Computational Details. All calculations were performed with the Gaussian09 suite of programs.[53] Prior to geometry optimization, dihedral scans were performed at a low level of theory (HF/3-21G) to approximate the global energy minimum conformation of molecular species containing easily rotating torsion angles. Optimizations of ground state geometries for global minimum conformations were then carried out to full convergence at the MP2/6-311+G(d,p)[54] and CBS-QB3[55] levels of theory. Single-point electronic energies were computed at the MP2/6-311+G(d,p) level using MP2 optimized geometries. Vibrational analyses were carried out at the CBS-QB3 level, and the

resulting frequencies were used for thermochemical calculations. Similar computational methodologies have been shown to be reliable for Diels–Alder reactions involving furan and maleimide.[49] Transition state searches were performed using the QST2 method[56] at the B3LYP/6-311G(d,p) level and then refined by Berny optimization at the MP2/6-31+G(d) and CBS-QB3 levels. Transition states were distinguished by having a single imaginary vibrational frequency corresponding to the vibrational mode that connects Diels–Alder adducts to their separated diene and dienophile components. Gas-phase single-point electronic energies for transition states were calculated at the MP2/6-31+G(d) level, with vibrational analysis being carried out at the CBS-QB3 level for zero-point and thermal corrections. Solvation free energies were calculated utilizing the PCM reaction field model[57] in acetonitrile (ε = 35.688).

Chemicals. Chemicals were obtained from commercial sources and used as purchased. Diels–Alder adducts of unsubstituted as well as derivatized furan and maleimide compounds were prepared according to literature procedures.[38]

^{1}H NMR Spectroscopic Studies. Dynamic exchange reactions were carried out directly in screw-cap NMR tubes. ^{1}H NMR spectra were obtained using a 300 MHz NMR spectrometer, and chemical shifts are reported as parts per million (ppm) downfield from the signal of Me_4Si. Equimolar amounts of an unsubstituted furan–maleimide Diels–Alder adduct and either *N*-methylmaleimide or 2-methylfuran were dissolved in 1.0 mL of CD_3CN in a screw-cap NMR tube to give a 0.25 M solution. The top of the NMR tube was then wrapped tightly in Teflon tape. An initial ^{1}H NMR spectrum was obtained at 298 K immediately after sample preparation and taken as time = 0 h. The NMR tube was then suspended in a stirred mineral oil bath kept at a constant 348 K, except when the sample was periodically removed from the oil bath and cooled to room temperature and an ^{1}H NMR spectrum was obtained. Such monitoring of the dynamic exchange process initially consisted of acquiring spectra at 1 h intervals, gradually ramping up to longer time intervals between acquisitions. The integration of diagnostic proton signals corresponding to different dynamic exchange products was used to evaluate the extent of exchange as a function of time.

■ ASSOCIATED CONTENT

Supporting Information. Figures, tables, and text giving time versus mole fraction plots for ^{1}H NMR dynamic exchange experiments, comparison of ^{1}H NMR spectra from dilute (0.25 M, 400 h equilibration) and concentrated (2.0 M, 24 h equilibration) dynamic exchange reactions, NMR spectra of adducts **14** and **15**, Cartesian coordinates of all stationary points reported in this paper and their absolute energies in hartrees, and the full author list for ref 53. This material is available free of charge via the Internet at http://pubs.acs.org.

■ AUTHOR INFORMATION

Corresponding Author

*E-mail: bnorthrop@wesleyan.edu.

■ ACKNOWLEDGMENT

We are grateful to the ACS PRF for financial support through a research grant to B.H.N. and to the ACS Physical Division Workshop for Undergraduate Students for a travel grant to R.C.B. We thank Wesleyan University for computer time supported by the NSF under Grant No. CNS-0619508. We thank Prof. George A. Petersson for helpful discussions.

■ REFERENCES

(1) Huc, I.; Lehn, J.-M. *Proc. Natl. Acad. Sci. U.S.A.* **1997**, *94*, 2106–2110.
(2) Ramstrom, O.; Lehn, J.-M. *Nat. Rev. Drug Discovery* **2002**, *1*, 26–36.
(3) Lehn, J.-M.; Eliseev, A. V. *Science* **2001**, *291*, 2331–2332.
(4) Rowan, S. J.; Santrill, S. J.; Cousins, G. R. L.; Sanders, J. K. M.; Stoddart, J. F. *Angew. Chem., Int. Ed.* **2002**, *41*, 898–952.
(5) Corbett, P. T.; Leclaire, J.; Vial, L.; West, K. R.; Wietor, J.-L.; Sanders, J. K. M.; Otto, S. *Chem. Rev.* **2006**, *106*, 3652–3711.
(6) Lehn, J.-M. *Angew. Chem., Int. Ed.* **1990**, *29*, 1304–1319.
(7) Lindsey, J. S. *New J. Chem.* **1991**, *15*, 153–180.
(8) Philp, D.; Stoddart, J. F. *Angew. Chem., Int. Ed.* **1996**, *35*, 1155–1196.
(9) Leininger, S.; Olenyuk, B.; Stang, P. J. *Chem. Rev.* **2000**, *100*, 853–908.
(10) Grzybowski, B.; Whitesides, G. W. *Science* **2002**, *295*, 2418–2421.
(11) See, for example: (a) Brady, P. A.; Bonar-Law, R. P.; Rowan, S. J.; Suckling, C. J.; Sanders, J. K. M. *Chem. Commun.* **1996**, 319–320. (b) Melson, G. A.; Busch, D. H. *J. Am. Chem. Soc.* **1964**, *86*, 213–217. (c) Otto, S.; Furlan, R. L. E.; Sanders, J. K. M. *Science* **2002**, *297*, 590–593. (d) Fuchs, B.; Nelson, A.; Star, A.; Stoddart, J. F.; Vidal, S. B. *Angew. Chem., Int. Ed.* **2003**, *42*, 4220–4224.
(12) Hubin, T. J.; Busch, D. H. *Coord. Chem. Rev.* **2000**, *200*, 5–52.
(13) Albrecht, M. *J. Inclusion Phenom. Macrocycl. Chem.* **2000**, *36*, 127–151.
(14) Wang, D. Y.; Mohwald, H. *J. Mater. Chem.* **2004**, *14*, 459–468.
(15) Meyer, C. D.; Joiner, C. S.; Stoddart, J. F. *Chem. Soc. Rev.* **2007**, *36*, 1705–1723.
(16) Glink, P. T.; Oliva, A. I.; Stoddart, J. F.; White, A. J. P.; Williams, D. J. *Angew. Chem., Int. Ed.* **2001**, *40*, 1870–1875.
(17) Leigh, D. A.; Lusby, P. J.; Teat, S. J.; Wilson, A. J.; Wong, J. K. Y. *Angew. Chem., Int. Ed.* **2001**, *40*, 1538–1543.
(18) (a) Williams, A. R.; Northrop, B. H.; Chang, T.; Stoddart, J. F.; White, A. J. P.; Williams, D. J. *Angew. Chem., Int. Ed.* **2006**, *45*, 6665–6669. (b) Northrop, B. H.; Aricó, F.; Tangchaivang, N.; Badjić, J. D.; Stoddart, J. F. *Org. Lett.* **2006**, *8*, 3899–3902.
(19) Chichak, K. S.; Cantrill, S. J.; Pease, A. R.; Chiu, S.-H.; Cave, G. W. V.; Atwood, J. L.; Stoddart, J. F. *Science* **2004**, *304*, 1308–1312.
(20) Pentecost, C. D.; Chichak, K. S.; Peters, A. J.; Cave, G. W. V.; Cantrill, S. J.; Stoddart, J. F. *Angew. Chem., Int. Ed.* **2007**, *46*, 218–222.
(21) (a) Côté, A. P.; Benin, A. L.; Ockwig, N. W.; O'Keeffe, M.; Matzger, A. J.; Yaghi, O. M. *Science* **2005**, *310*, 1166–1170. (b) El-Kaderi, H. M.; Hunt, J. R.; Mendoza-Cortes, J. L.; Côté, A. P.; Taylor, R. E.; O'Keeffee, M.; Yaghi, O. M. *Science* **2007**, *316*, 268–272.
(22) (a) Kuhn, P.; Antonietti, M.; Thomas, A. *Angew. Chem., Int. Ed.* **2008**, *47*, 3450–3453. (b) Thomas, A. *Angew. Chem., Int. Ed.* **2010**, *49*, 8328–8344 and references therein.
(23) (a) Tilford, R. W.; Gemmill, W. R.; zur Loye, H. C.; Lavigne, J. J. *Chem. Mater.* **2006**, *18*, 5296–5301. (b) Tilford, R. W.; Mugavero, S. J.; Pellechia, P. J.; Lavigne, J. J. *Adv. Mater.* **2008**, *20*, 2741–2746.
(24) (a) Spitler, E.; Dichtel, W. R. *Nature Chem.* **2010**, *2*, 672–677. (b) Colson, J. W.; Woll, A. R.; Mukherjee, A.; Levendorf, M. P.; Spitler, E. L.; Shields, V. B.; Spencer, M. G.; Park, J.; Dichtel, W. R. *Science* **2011**, *332*, 228–231. (c) Spitler, E. K.; Giovino, M. R.; White, S. L.; Dichtel, W. R. *Chem. Sci.* **2011**, *2*, 1588–1593.
(25) (a) Christinat, N.; Scopelliti, R.; Severin, K. *J. Org. Chem.* **2007**, *72*, 2192–2200. (b) Christinat, N.; Scopelliti, R.; Severin, K. *Angew. Chem., Int. Ed.* **2008**, *47*, 1848–1852. (c) Christinat, N.; Scopelliti, R.; Severin, K. *Chem. Commun.* **2008**, 3660–3662.
(26) (a) Nitschke, J. R. *Acc. Chem. Res.* **2007**, *40*, 103–122. (b) Hutin, M.; Bernardinelli, G.; Nitschke, J. R. *Chem. Eur. J.* **2008**, *14*, 4585–4593. (c) Campbell, V. E.; de Hatten, X.; Delsuc, N.; Kauffmann, B.; Huc, I.; Nitschke, J. R. *Nature Chem.* **2010**, *2*, 684–687.
(27) Sauer, J.; Sustmann, R. *Angew. Chem., Int. Ed., Engl.* **1980**, *19*, 779–807.
(28) (a) Chen, X.; Dam, M. A.; Ono, K.; Mal, A.; Shen, H.; Nutt, S. R.; Sheran, K.; Wudl, F. *Science* **2002**, *295*, 1698–1792. (b) Chem, X.;

Wudl, F.; Mal, A. K.; Shen, H.; Nutt, S. R. *Macromolecules* **2003**, *36*, 1802–1807.
(29) (a) McElhanon, J. R.; Wheeler, D. R. *Org. Lett.* **2001**, *3*, 2681–2683. (b) Szalai, M. L.; McGrath, D. V.; Wheeled, D. R.; Zifer, T.; McElhanon, J. R. *Macromolecules* **2007**, *40*, 818–823. (c) Polasket, N. W.; McGrath, D. V.; McElhanon, J. R. *Macromolecules* **2011**, *44*, 3203–3210.
(30) Merve Kose, M.; Yesilgad, G.; Sanyal, A. *Org. Lett.* **2008**, *10*, 2353–2356.
(31) Vieyres, A.; Lam, T.; Gillet, R.; Franc, G.; Castonguay, A.; Kakkar, A. *Chem. Commun.* **2010**, 1875–1877.
(32) McElhanon, J. R.; Zifer, T.; Kline, S. R.; Wheeler, D. R.; Loy, D. A.; Jamison, G. M.; Long, T. M.; Rahimian, K.; Simmons, B. A. *Langmuir* **2005**, *21*, 3259–3266.
(33) Tian, Q.; Yuan, Y. C.; Rong, M. Z.; Zhang, M. Q. *J. Mater. Chem.* **2009**, *19*, 1289–1296.
(34) Zhang, Y.; Broekhuis, A. A.; Picchioni, F. *Macromolecules* **2009**, *42*, 1906–1912.
(35) Adzima, B.; Aguirre, H. A.; Kloxin, C. J.; Scott, T. F.; Bowman, C. N. *Macromolecules* **2008**, *41*, 9112–9117.
(36) Reutenauer, P.; Buhler, E.; Boul, P. J.; Candau, S. J.; Lehn, J.-M. *Chem. Eur. J.* **2009**, *15*, 1893–1900.
(37) (a) Liu, X.; Zhu, M.; Chen, S.; Yuan, M.; Guo, Y.; Song, Y.; Liu, H.; Li, Y. *Langmuir* **2008**, *24*, 11967–11974. (b) Liu, X.; Liu, H.; Zhou, W.; Zheng, H.; Yin, X.; Li, Y.; Guo, Y.; Zhu, M.; Ouyang, C.; Zhu, D.; Xia, A. *Langmuir* **2010**, *26*, 3179–3185.
(38) Zhu, J.; Kell, A. J.; Workentin, M. S. *Org. Lett.* **2006**, *8*, 4993–4996.
(39) Bahman, A.; Bakhtiari, S.; Hsiao, D.; Jin, G.; Gates, B. D.; Branda, N. *Angew. Chem., Int. Ed.* **2009**, *48*, 4166–4169.
(40) Lemieux, V.; Gauthier, S.; Branda, N. R. *Angew. Chem., Int. Ed.* **2006**, *45*, 6820–6824.
(41) Boul, P. J.; Reutenauer, P.; Lehn, J.-M. *Org. Lett.* **2005**, *7*, 15–18.
(42) Kotha, S.; Banerjee, S.; Patil, M. P.; Sunoj, R. B. *Org. Biomol. Chem.* **2006**, *4*, 1854–1856.
(43) Jones, G. O.; Houk, K. N. *J. Org. Chem.* **2008**, *73*, 1333–1342.
(44) Reutenauer, P.; Boul, P. J.; Lehn, J.-M. *Eur. J. Org. Chem.* **2009**, 1691–1697.
(45) Pieniazek, S. N.; Houk, K. N. *Angew. Chem., Int. Ed.* **2006**, *45*, 1442–1445.
(46) Kwart, H.; Burchuk, I. *J. Am. Chem. Soc.* **1952**, *74*, 3094–3097.
(47) Berson, J.; Swidler, R. *J. Am. Chem. Soc.* **1954**, *76*, 4060–4069.
(48) Goh, Y. W.; Pool, B. R.; White, J. M. *J. Org. Chem.* **2008**, *73*, 151–156.
(49) Rulísek, L.; Sebek, P.; Havlas, Z.; Hrabal, R.; Capek, P.; Svatos, A. *J. Org. Chem.* **2005**, *70*, 6295–6302.
(50) Tobia, D.; Harrison, R.; Phillips, B.; White, T. L.; DiMare, M.; Rickborn, B. *J. Org. Chem.* **1993**, *58*, 6701–6706.
(51) Guner, V.; Khuong, K. S.; Leach, A. G.; Lee, P. S.; Bartberger, M. D.; Houk, K. N. *J. Phys. Chem. A* **2003**, *107*, 11445–11459.
(52) This ratio is based upon a Boltzmann distribution (at 348 K) taking into account the relative free energies calculated for the four products at equilibrium: **16**-*exo* (−4.5 kcal/mol), **9**-*exo* (−3.6 kcal/mol), **16**-*endo* (−1.5 kcal/mol), and **9**-*endo* (−1.1 kcal/mol). Contributions of both exo and endo isomers of each adduct were combined to arrive at the total 22:78 ratio for **9**:**16**.
(53) Frisch, M. J. et al. *Gaussian 09, Revision A.1* (see the Supporting Information for the full reference).
(54) (a) Frisch, M. J.; Head-Gordon, M.; Pople, J. A. *Chem. Phys. Lett.* **1990**, *166*, 275–280. (b) Frisch, M. J.; Head-Gordon, M.; Pople, J. A. *Chem. Phys. Lett.* **1990**, *166*, 281–289.
(55) (a) Nyden, M. R.; Petersson, G. A. *J. Chem. Phys.* **1981**, *75*, 1843–1862. (b) Petersson, G. A.; Al-Laham, M. A. *J. Chem. Phys.* **1991**, *94*, 6081–6090. (c) Petersson, G. A.; Tensfeldt, T.; Montgomery, J. A. *J. Chem. Phys.* **1991**, *94*, 6091–6101. (d) Montgomery, J. A.; Ochterski, J. W.; Petersson, G. A. *J. Chem. Phys.* **1994**, *101*, 5900–5909.
(56) Peng, C.; Ayala, P. Y.; Schlegel, H. B.; Frisch, M. J. *J. Comput. Chem.* **1996**, *17*, 49–56.
(57) (a) Miertus, S.; Scrocco, E.; Tomasi, J. *Chem. Phys.* **1981**, *55*, 117–129. (b) Cossi, M.; Barone, V.; Cammi, R.; Tomasi, J. *Chem. Phys. Lett.* **1996**, *255*, 327–335.